JOURNAL OF MATERIALS SCIENCE 28 (1993) 5894–5900

Dielectric spectroscopy of $MgTiO_3$-based ceramics in the 10^9–10^{14} Hz region

V. M. FERREIRA, J. L. BAPTISTA
Departamento de Engenharia Cerâmica e Vidro/INESC, Universidade de Aveiro, 3800 Aveiro, Portugal

S. KAMBA, J. PETZELT
Institute of Physics, Czechoslovak Academy of Sciences, Na Slovance 2, 18040 Prague 8, Czechoslovakia

Magnesium titanate ($MgTiO_3$) powder was prepared by a chemical route (Pechini method) and different dopants were added to prepare several compositions. These pure and doped compositions were sintered in air and dense ceramics were obtained. The pure $MgTiO_3$ samples were also subjected to different heat treatments during sintering. Complex permittivity spectra of ceramic samples were determined by various techniques in the 10^9–10^{14} Hz range. These techniques included infrared spectroscopy in transmission and reflectivity modes and microwave dielectric measurements. Extrapolation to microwave frequencies from infrared data, according to the proportionality $\varepsilon''(\nu) \propto \nu$, agrees quite well with the microwave data measured at 8 GHz and it is a useful procedure to estimate intrinsic microwave losses. Fast cooling from high temperatures of $MgTiO_3$ samples increased dielectric loss, probably due to a structural disorder. Dopants have two types of effect depending on whether they form a distinct second phase or a solid solution with $MgTiO_3$. In this last case intrinsic losses are strongly affected.

1. Introduction

There have been some recent attempts to use far infrared spectroscopy to help in the characterization of the dielectric properties of some low lossy materials in the microwave region [1–3]. This was based on work developed since 1960 on some ferroelectric materials, where permittivity and dielectric losses were calculated from infrared spectra and correlated with the existence of polar lattice vibration modes [4–6].

Losses in microwave dielectrics can be classified as intrinsic and extrinsic, the first representing the minimum that can be expected for a particular material composition, independent of the processing conditions and microstructure. In the far infrared region (10^{12}–10^{13} Hz) the intrinsic factors play a fundamental role since the intrinsic dielectric losses are much stronger than the extrinsic ones [3, 7–9]. In principle, it should therefore be possible to extract the value of the intrinsic losses in the microwave region from the infrared data if the extrapolation law is known. Intrinsic losses exist even in a perfect lattice and they are related to anharmonicity of its vibration modes. The anharmonicity of the lattice vibrations can be characterized in the simplest way as one-phonon absorption lines, with finite damping constants leading to nonzero dielectric losses. The extrinsic losses are related to mechanisms dependent on lattice imperfections, such as defects (vacancies, impurities), structural disorder or microstructure (processing faults, porosity, second phases). These mechanisms predominate at frequencies lower than the far infrared where the intrinsic losses are small.

The complex dielectric response in the region of one-phonon absorption bands is in the simplest case modelled by an additive system of damped harmonic oscillators:

$$\varepsilon^* = \varepsilon_\infty + \sum_{i=1}^{n} \frac{S_i}{\nu_i^2 - \nu + i\nu\gamma_i} \quad (1)$$

where ν_i, γ_i and S_i are the eigenfrequency, damping and strength of the ith polar lattice mode, respectively, and ε_∞ is the real permittivity due to higher frequency absorption processes. Extrapolating this model to frequencies $\nu \ll \nu_i$ gives,

$$\varepsilon' = \varepsilon_\infty + \sum_{i=1}^{n} \frac{S_i}{\nu_i^2} \quad (2)$$

and

$$\varepsilon'' = \nu \sum_{i=1}^{n} \frac{S_i\gamma_i}{\nu_i^4} \quad (3)$$

i.e. frequency-independent permittivity and losses proportional to frequency. Also, the microscopic theory of dielectric losses [9] leads to $\varepsilon'' \propto \nu$ for $\nu \ll \nu_i$ but the proportionality constant might not be precisely that of Equation 3. All reliable experimental results on well processed samples so far published [1, 2, 10] show that the losses extrapolated by Equation 3 give slightly

0022–2461

lower microwave values than actually measured, but of the same order of magnitude. Therefore the extrapolation can be used to predict the ultimate intrinsic microwave losses.

Experimentally, the only technique which enables the determination of the dielectric response in the high absorption region is the measurement of the bulk reflectivity spectra $R(\nu)$. The lattice mode parameters are mostly obtained by a fit to Equation 1 using a well known relation between R and ε^*:

$$R = \left(\frac{\sqrt{\varepsilon^*} - 1}{\sqrt{\varepsilon^*} + 1}\right)^2 \quad (4)$$

In the low frequency range $\nu \ll \nu_i$ the sample may become transparent for a reasonable thickness (0.1–1 mm) and transmission spectroscopy is more useful and accurate. Then the dielectric response may be obtained from the interference pattern of the transmitted radiation through a plane parallel plate directly, without assuming any model [11].

It is possible to predict the number of active vibration modes present in the reflectivity spectra through the analysis of the crystallographic structure. $MgTiO_3$ has the ilmenite type structure, belonging to the trigonal space group $R\bar{3}$ $\{Z = 2(6)\}$. The Mg^{2+} and Ti^{4+} ions occupy trigonal $2c3$ sites, whereas O^{2-} ions sit on general $6f1$ sites. The factor-group analysis reveals the following decomposition of the vibrational representation in the Brillouin zone centre:

$$\Gamma_v = 5A_g + 5A_u + 5E_g + 5E_u \quad (5)$$

in which the $4A_u$ and $4E_u$ optical modes are infrared active. The other $1A_u$ and $1E_u$ represent the acoustic modes and the other modes are Raman active.

In ceramic samples, one should also take into account that anisotropy of infrared reflectivity may lead to effective broadening of some modes and effective changes of infrared mode strength caused by averaging of different spectra.

The main purpose of this work is to better understand the mechanisms responsible for the dielectric losses in ceramics of magnesium titanate ($MgTiO_3$), in the microwave frequency region (10^9 Hz). It is important for the application of these ceramics as dielectric resonators that they show very low dielectric losses in that range [12]. The understanding of these mechanisms will permit the design of better materials.

In order to know the influence of several factors on the total losses of the $MgTiO_3$-based compositions, we prepared samples with different additives and also with different heat treatments and studied their infrared spectra in correlation with the microwave losses.

2. Experimental procedure

The $MgTiO_3$ powder used for the several compositions was prepared by a chemical route (Pechini method). In this method the titanium precursor is a solution of tetraethylorthotitanate and citric acid in ethyleneglycol, while the magnesium precursor is a precipitated magnesium carbonate. The magnesium carbonate was dissolved, by reaction with nitric acid, into the titanium solution. This final solution was then dried in several steps up to a maximum temperature of 250 °C. This procedure yielded a polyester resin which, by calcination at 600 °C, gave a single phase $MgTiO_3$ powder. The powder was then ballmilled for 16 h using nylon vials with agate balls.

Powders for the different compositions (Table I) were isostatically pressed at 2000 Kgf cm^{-2} into pellets of 10 mm diameter. Most of these pellets were sintered in air at 1350 °C for 2 h. The heating and cooling rate was 5 °C min^{-1}, except for samples 2 and 3 which were cooled at a much faster rate (air-quenched). Also, for sample 3 the sintering temperature was different (1500 °C). Table I lists the different samples used in this study, their sintering conditions and the densification values achieved after sintering.

The dopants were added to the $MgTiO_3$ powder and mixed with it by a wet milling process (2 h). The amounts of all dopants used are expressed as molar %. Samples 1–3 are single phase $MgTiO_3$ without any dopant. Samples 4–6 are doped with Nb^{5+} through addition of Nb_2O_5. Sample 7 is doped with La^{3+}, using La_2O_3 as a precursor. Samples 8 and 9 are doped with $CaTiO_3$, which was also prepared by the Pechini method. Samples 10–12 are doped with Cr^{3+}, Co^{2+} and Ni^{2+} by the respective additions of Cr_2O_3, CoO and NiO. Finally, samples 13 and 14 were prepared with a deviation of stoichiometry with

TABLE I Samples characteristics

Sample	Sample composition	Sintering conditions	D_s^a(%)
1	$MgTiO_3$	1350 °C/2 h (5 °C min^{-1})	96.8
2	$MgTiO_3$	1350 °C/2 h (quenched)	97.0
3	$MgTiO_3$	1500 °C/2 h (quenched)	97.0
4	$MgTiO_3$ + 0.5% Nb^{5+}	1350 °C/2 h (5 °C min^{-1})	97.0
5	$MgTiO_3$ + 1.0% Nb^{5+}	1350 °C/2 h (5 °C min^{-1})	97.0
6	$MgTiO_3$ + 2.0% Nb^{5+}	1350 °C/2 h (5 °C min^{-1})	96.0
7	$MgTiO_3$ + 1.0% La^{3+}	1350 °C/2 h (5 °C min^{-1})	99.0
8	96% $MgTiO_3$ + 4% $CaTiO_3$	1350 °C/2 h (5 °C min^{-1})	96.5
9	94% $MgTiO_3$ + 6% $CaTiO_3$	1350 °C/2 h (5 °C min^{-1})	96.8
10	$MgTiO_3$ + 1.0% Cr^{3+}	1350 °C/2 h (5 °C min^{-1})	97.0
11	$MgTiO_3$ + 1.0% Co^{2+}	1350 °C/2 h (5 °C min^{-1})	97.5
12	$MgTiO_3$ + 1.0% Ni^{2+}	1350 °C/2 h (5 °C min^{-1})	97.8
13	$MgTiO_3$(+ 2% MgO)	1350 °C/2 h (5 °C min^{-1})	98.0
14	$MgTiO_3$(+ 4% MgO)	1350 °C/2 h (5 °C min^{-1})	97.3

[a] Densification.

excess MgO, which was induced during chemical preparation of the powders.

The densities of the sintered pellets were determined by a liquid immersion method. X-ray diffraction techniques were used to analyze the powders and products. Microstructure of sintered samples was studied by scanning electron microscopy (SEM) and analyzed by energy dispersive spectroscopy (EDS).

Microwave dielectric properties were determined at 8 GHz by the Hakki and Coleman technique [13]. Fourier transform infrared spectroscopy (FTIRS) was performed, in transmission and reflection modes, using a Bruker IFS 113v spectrometer. The samples were dense ceramic discs carefully polished to ensure flat and plane parallel surfaces. The samples for transmission and reflectivity had thicknesses of around 0.3 and 1 mm, respectively. Both of them were about 7 mm in diameter.

All the FTIR measurements were done at 300 K, with the spectrometer evacuated to 2.026×10^3 Pa in order to prevent any infrared absorption by gas molecules. Nearly normal reflectivity (11°) was measured between 30 and 3000 cm^{-1} (10^{12}–10^{14} Hz) using three beamsplitters with different spectral ranges of transmission and ratioed to a gold mirror reference. The several curves obtained were automatically merged. Transmission was measured in a lower range (15–100 cm^{-1}) with two beamsplitters. For this range of frequencies, a He-cooled Ge bolometer was used as a detector.

The reflectivity spectra were fitted to the sum of the classical damped oscillator model to obtain the complex permittivity function, $\varepsilon^*(\nu) = \varepsilon'(\nu) - i\varepsilon''(\nu)$.

For the transmission measurements the ε' and ε'' calculations were carried out on the maxima of the obtained interference pattern [11].

3. Results and discussion

Fig. 1 shows a typical reflectivity spectrum of a $MgTiO_3$ ceramic (sample 1). The fit also shown in Fig. 1 was performed with six oscillators, distinctly seen in the spectra. Minor features in the reflectivity spectra (requiring additional weak oscillators for the fit) were neglected, as they do not appreciably influence the low-frequency part which is our main interest. Indeed, as can be seen from Fig. 2, the major contribution comes from the two lowest modes revealed on the spectra. This was the reason why great care was especially taken in the fitting of these first two modes, because slight differences in the dispersion parameters significantly affect the dielectric losses and their extrapolation to lower frequencies.

Generally, all the spectra exhibit six vibration modes located at the following approximate frequencies: 278, 321, 420, 472, 529 and 620 cm^{-1}. The first two modes probably correspond to the cation vibration modes inside the oxygen octahedra. Because titanium is heavier than magnesium, we assign the first mode to (Ti–O_6) vibrations, while the second one may probably be predominantly related to the (Mg–O_6) vibration in the lattice. The exact assignment of vibration modes is complex and requires the elaboration of a microscopic model.

Fig. 3 shows the $\varepsilon''(\nu)$ spectra on a logarithmic scale, calculated from reflectivity of sample 1, as well as the

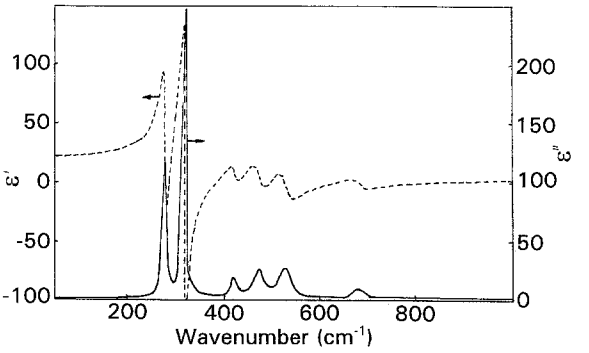

Figure 2 Permittivity (ε' dashed line) and loss factor (ε'' solid line) spectra derived from the fitting curve in Fig. 1.

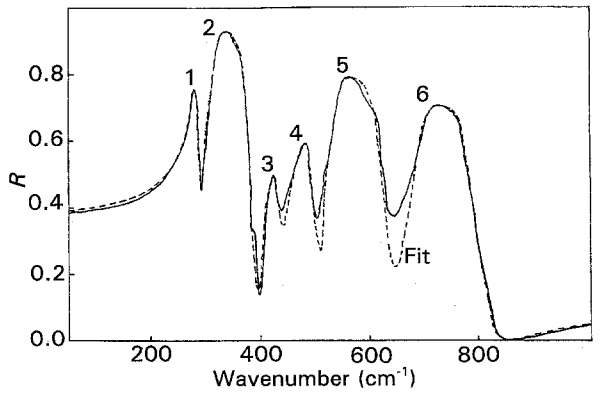

Figure 1 Reflectivity spectrum of pure $MgTiO_3$ (sample 1) and fitted curve (dashed line). The parameters (ν_i, γ_i and S_i) used to fit the six oscillators of the R spectrum were in the same order: 1 (278; 6; 460^2); 2 (321; 8; 840^2); 3 (420; 20; 370^2); 4 (472; 26; 540^2); 5 (529; 33; 670^2); 6 (680; 37; 490^2); with $\varepsilon_\infty = 5.0$.

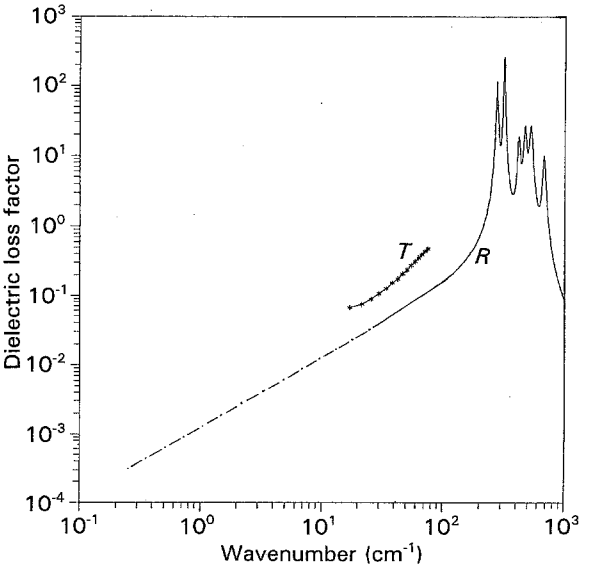

Figure 3 Dielectric loss factor (ε'') spectra of pure $MgTiO_3$ (sample 1) by transmission (T) and reflectivity (R) modes; The point-dashed line indicates extrapolation performed from the R curve down to microwave frequencies.

linear extrapolation to lower frequencies. The extrapolation gives a straight line with a slope of 1, since for $\nu \ll \nu_i$ we have $\varepsilon'' \propto \nu$. The calculation of the losses in the one-phonon absorption region is not very accurate and the extrapolation might introduce an error of about 30% [10]. Nevertheless, there has been good coherence between the values obtained by extrapolation to lower frequencies and the ones measured at such frequencies by other methods [1, 2, 10].

In order to decrease the error and extend the data to lower frequencies, transmission measurements were also performed, because they allow a more accurate calculation of ε' and ε'' in the low frequency range (15–100 cm^{-1}). The ε'' spectrum of sample 1 calculated from transmission data is also presented in Fig. 3. In the system of complex perovskites [10], the losses extrapolated from reflectivity were always two to five times lower than the ones calculated from transmission measurements. The same effect was observed here for all the tested samples of pure and doped $MgTiO_3$. This might be due to the fact that some extrinsic contributions start to play a role at these frequencies, but also the simple linear extrapolation may break down for $\nu \ll \nu_i$, even in the ideal single crystal [9].

Figs 4–9 show the dielectric spectra for the several samples calculated from the reflectivity and transmission measurements, as well as the linear extrapolation performed to the microwave region (0.27 cm^{-1}/8 GHz). It also shows the microwave dielectric measurements made by the Hakki and Coleman technique at the same frequency (8 GHz). Table II presents the values of microwave permittivity and dielectric losses corresponding to Figs 4–9.

Before discussion of particular cases some common aspects present in all transmission spectra should be referred to. A slope of 1 was found for the variation of ε'' with frequency (logarithmic scale) up to 40–50 cm^{-1}. Above 40–50 cm^{-1} the theoretically expected quadratic relationship ($\varepsilon'' \propto \nu^2$) [9] is approached, with slopes of 1.3–1.7 measured for the different curves. Most of these transmission curves present a slight deviation from linearity at frequencies lower than 20 cm^{-1}. This deviation is probably due to the fact that transmission values are already too high (≈ 1.0), which causes an error on the calculation of ε' and ε''.

Generally, we can say that there is a good agreement in relative terms between the results extrapolated from transmission and reflectivity data and the microwave measurements. However, the extrapolation shows that some part of the microwave (and maybe submillimeter) losses might be of extrinsic origin. One possible way to separate extrinsic and intrinsic losses is to measure temperature dependences of loss spectra.

Samples 1, 2 and 3 are dense ceramics of single phase $MgTiO_3$ as revealed by SEM/EDS. Examining the dielectric losses of these undoped $MgTiO_3$ samples, which are presented in Fig. 4, it can be seen that the increase in losses previously detected for sample 3 by microwave measurements [14] is confirmed by the

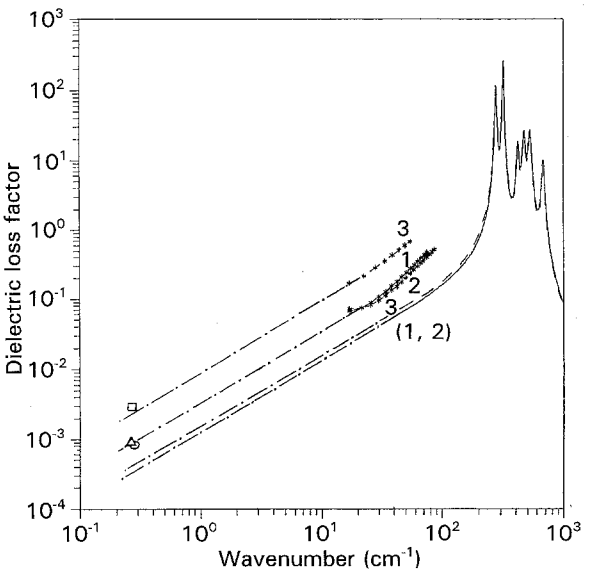

Figure 4 Dielectric spectra of samples 1, 2 and 3. The point-dashed line represents extrapolation according to $\varepsilon''(\nu) \propto \nu$ down to 8 GHz (0.267 cm^{-1}). Measured microwave data is also shown in the figure (△ sample 1; ○ sample 2; □ sample 3).

TABLE II Permittivity and dielectric losses of $MgTiO_3$-based ceramics (at 8 GHz)

Sample composition	Sample	ε_r (Mw)	ε_r (Tr)	ε_r (R)	tan δ (Mw) ($\times 10^{-5}$)	tan δ (Tr) ($\times 10^{-5}$)	tan δ (R) ($\times 10^{-5}$)
MT1350	1	17.4	16.6	18.8	4.8	4.8	1.8
MT1350–AQ	2	17.7	16.7	18.8	4.5	4.8	1.8
MT1500–AQ	3	16.1	15.5	17.9	15.8	14.0	2.3
MT + 0.5% Nb^{5+}	4	17.7	16.9	18.3	4.8	4.8	2.3
MT + 1.0% Nb^{5+}	5	17.7	16.7		4.6	4.5	
MT + 2.0% Nb^{5+}	6	16.9	16.0	17.0	15.0	10.0	2.2
MT + 1.0% La^{3+}	7	18.1	17.6	19.3	17.0	6.1	2.0
96% MT + 4% CT	8	19.1	18.0		9.4	5.8	
94% MT + 6% CT	9	19.9	18.3	19.1	12.0	9.0	2.1
MT + 1.0% Cr^{3+}	10	17.4	16.6	17.5	6.7	9.7	2.1
MT + 1.0% Co^{2+}	11	17.4	17.0	17.5	5.8	6.0	2.7
MT + 1.0% Ni^{2+}	12	17.4	16.7	16.1	6.0	6.0	3.0
MT(+ 2% MgO)	13	17.3	16.6	18.9	4.6	6.4	2.0
MT(+ 4% MgO)	14	17.2	16.3	18.6	5.1	4.1	2.7

Mw: microwave; Tr: transmission; R: reflection.

results extrapolated from transmission and reflectivity data. A structural disorder induced by fast cooling from temperatures above 1400 °C was suggested as a possible cause for the observed increase [14]. A structural disorder phenomena can indeed modify the vibration modes damping constant or activate other phonons by breaking the translational symmetry, leading to an increase of dielectric losses. It is doubtful that extrinsic microstructure factors could be responsible for such an increase, since all samples have the same porosity and fast cooling would have affected samples 2 and 3 in the same way. Another possible concurrent extrinsic factor would be the localized hopping of charged defects (vacancies, impurities). Oxygen vacancies created by an eventual reduction due to the fast cooling of the samples could be a possibility. However, these defects are not likely to be present at frequencies above 10^{11} Hz ($> 30\ cm^{-1}$) and so have no appreciable influence on the far infrared losses [3].

For doped $MgTiO_3$ samples two different situations are present. In one of them the dopant is in solid solution and in the other one the solid solution limit has been exceeded and two phases are therefore present.

For the Nb^{5+}-doped $MgTiO_3$ (samples 4–6) two phases can be detected by SEM for samples doped with 1.0 and 2.0 mol %, the second one being identified as niobium oxide by EDS analysis. In the sample doped with 0.5 mol % of Nb^{5+} no second phase could be detected either by XRD or by SEM observation, although EDS analysis revealed that some grains were richer in Nb^{5+} than others. As can be seen in Table I, the degree of densification of the samples was not modified by the presence of Nb^{5+}.

Fig. 5 shows the dielectric spectra of the Nb^{5+}-doped samples as well as the extrapolation for lower frequencies (8 GHz) and the measured microwave losses. The presence of the second phase in sample 6 was responsible for the great increase in the measured microwave losses. An increase in losses was also observed from the transmission measurements.

Sample 7 represents the composition of $MgTiO_3$ doped with 1% La^{3+}. The information obtained by SEM/EDS revealed that the presence of La^{3+}, even in small amounts (0.5%), causes the formation of a second phase, which is a lanthanum titanate. This must be related to the fact that La^{3+} is a rather large cation compared with Mg^{2+} and Ti^{4+}, and so it would be difficult for it to go into the lattice.

Fig. 6 shows the dielectric spectra of an La^{3+}-doped sample and also of sample 1 for comparison. The second phase formed by the introduction of La^{3+} is probably responsible for the increase in microwave losses, causing the same type of behaviour as described for the sample doped with Nb^{5+} and containing two phases. The extrapolated losses from reflectivity and transmission also increase, but on a minor scale. Transmission data also show an absorption band near $50\ cm^{-1}$, probably related to a resonant mode introduced by defects created by the presence of La^{3+}. So the fact that microwave losses are higher than those extrapolated from transmission may be related to this extrinsic contribution, which may have a nonlinear dependence with frequency.

Samples 8 and 9 represent compositions of $MgTiO_3$ doped with 4 and 6% $CaTiO_3$. This additive is normally used in order to bring to zero the temperature coefficient of the resonance frequency of $MgTiO_3$, although it increases both dielectric losses and permittivity [15]. $CaTiO_3$ presents at microwave frequencies high losses and also a high value of permittivity (≈ 160). Still, according to Tamura *et al.* [15], the introduction of La^{3+} in $MgTiO_3$–$CaTiO_3$ compositions will improve sintering and hence cause a decrease in dielectric losses. In the presence of $CaTiO_3$, La^{3+} will preferentially form a solid solution with that titanate. However, if La^{3+} should be in excess, a

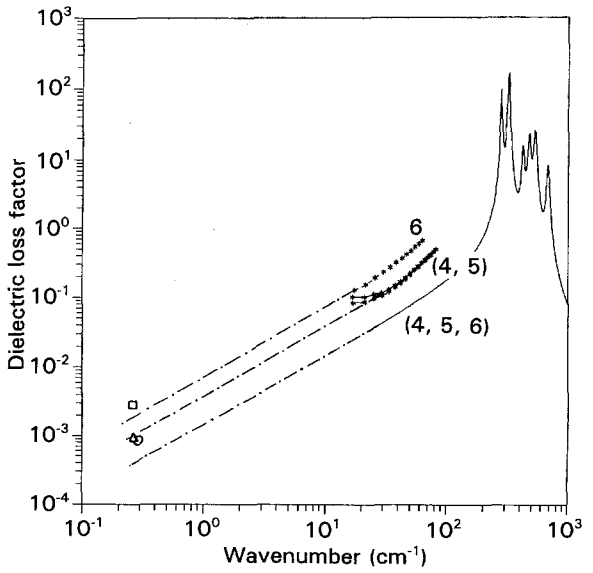

Figure 5 Dielectric spectra of samples 4, 5 and 6. The point-dashed line represents extrapolation according to $\varepsilon''(\nu) \propto \nu$ down to 8 GHz (0.267 cm^{-1}). Measured microwave data is also shown in the figure (△ sample 4; ○ sample 5; □ sample 6).

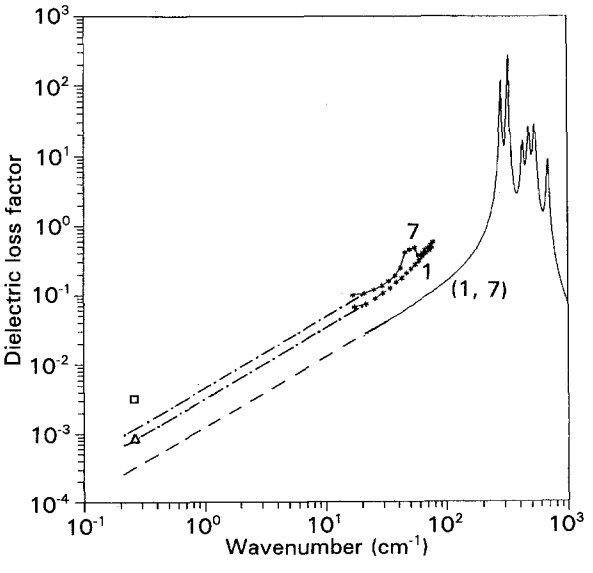

Figure 6 Dielectric spectra of samples 1 and 7. The point-dashed line represents extrapolation according to $\varepsilon''(\nu) \propto \nu$ down to 8 GHz (0.267 cm^{-1}). Measured microwave data is also shown in the figure (△ sample 1; □ sample 7).

second phase will be formed and dielectric losses will increase.

In the case of $CaTiO_3$ doping, observations by SEM and analysis by EDS clearly reveal the presence of a second phase identified as $CaTiO_3$. Its introduction did not change the densification behaviour of $MgTiO_3$.

Fig. 7 shows the data related to the $MgTiO_3$–$CaTiO_3$ compositions. The presence of $CaTiO_3$ causes an increase in losses measured at microwave frequencies, which is consistent with the increase in extrapolated values from transmission spectra. $CaTiO_3$ does not form a solid solution with $MgTiO_3$ and the final dielectric properties are the result of a mixing rule of the individual properties of the two titanates. In the reflectivity spectra a set of bands appears around 160 cm^{-1}, which are due to characteristic vibration modes of $CaTiO_3$. Their presence contributes to the small increase in intrinsic losses extrapolated from the reflectivity spectra.

Samples 10–12 represent compositions of $MgTiO_3$ doped with 1 mol % of Cr^{3+}, Co^{2+} and Ni^{2+}, respectively. These dopants were chosen with the purpose of constituting a solid solution with $MgTiO_3$. The main reason for their choice as dopants was the fact that they have a similar or identical crystallographic structure to $MgTiO_3$. While $CoTiO_3$ and $NiTiO_3$ belong to the same subgroup (ilmenite) as $MgTiO_3$, Cr_2O_3 belongs to a subgroup (corundum) of the same general group of structures. The difference resides in the fact that Cr^{3+} occupies in the lattice the relative positions of both Mg^{2+} and Ti^{4+}.

Haider *et al.* [16] performed several EPR measurements on $MgTiO_3$ single crystals, pure and doped with different transition metals including Cr^{3+}, Co^{2+} and Ni^{2+}. They came to the conclusion that indeed Co^{2+} and Ni^{2+} substitute Mg^{2+} ions, while for Cr^{3+} ions two positions in the lattice were equally possible. One associated with Mg^{2+} and the other one associated with Ti^{4+}.

Analysis by SEM/EDS showed that no second phase was formed with any of the dopants. Also, the densification was not significantly altered by their presence.

Fig. 8 presents the results related to these dopants. Their difference in lattice position and charge may justify the fact that Cr^{3+}-doped $MgTiO_3$ has higher losses than Co^{2+}- and Ni^{2+}-doped $MgTiO_3$ at microwave frequencies. The relative trend of measured values is followed by the values extrapolated from transmission data, although with some differences in absolute values. It can be said that Co^{2+} and Ni^{2+} do

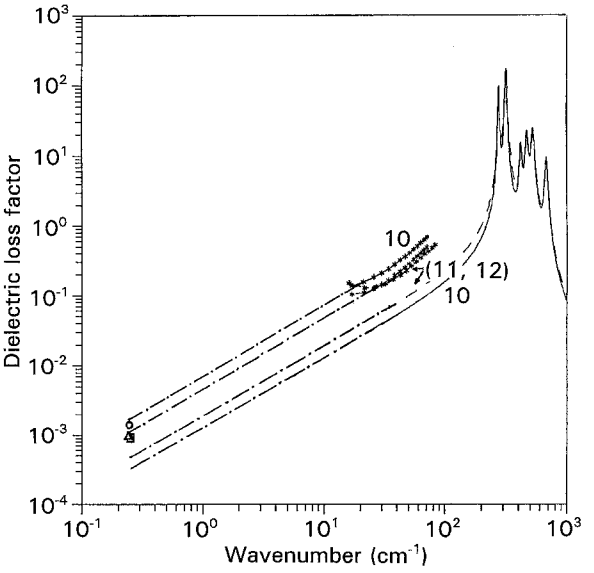

Figure 8 Dielectric spectra of samples 10–12. The point-dashed line represents extrapolation according to $\varepsilon''(\nu) \propto \nu$ down to 8 GHz (0.267 cm^{-1}). Measured microwave data is also shown in the figure (○ sample 10; △ sample 11; □ sample 12).

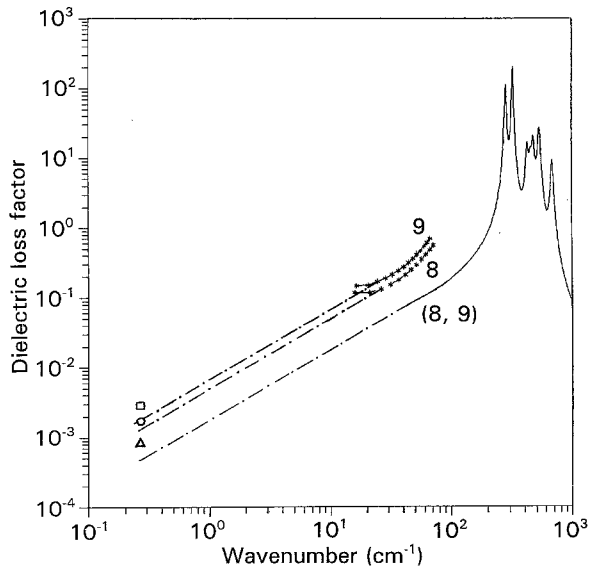

Figure 7 Dielectric spectra of samples 8 and 9. The point-dashed line represents extrapolation according to $\varepsilon''(\nu) \propto \nu$ down to 8 GHz (0.267 cm^{-1}). Measured microwave data is also shown in the figure (△ sample 1; ○ sample 8; □ sample 9).

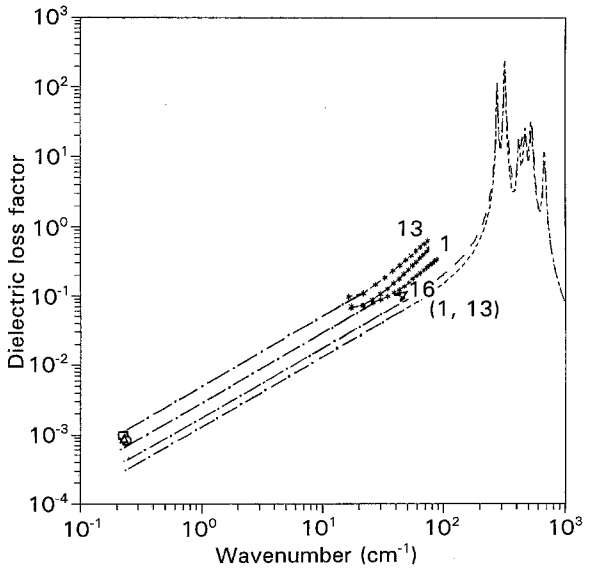

Figure 9 Dielectric spectra of samples 1, 13 and 14. The point-dashed line represents extrapolation according to $\varepsilon''(\nu) \propto \nu$ down to 8 GHz (0.267 cm^{-1}). Measured microwave data is also shown in the figure (△ sample 1; ○ sample 13; □ sample 14).

not cause significant changes in the lattice to alter the dielectric losses, while Cr^{3+} does.

Finally, samples 13 and 14 represent the compositions of $MgTiO_3$ with an induced deviation in stoichiometry of 2% and 4% of excess MgO, respectively.

Observation and analysis by SEM/EDS revealed that sample 13 does not present any second phase, while in sample 14 a minor phase was identified which is a magnesium titanate richer in magnesium (Mg_2TiO_4). The degree of densification of the samples was not altered by these modifications.

Fig. 9 presents the dielectric spectra of these samples and also of sample 1 for comparison. The increase in losses extrapolated from reflectivity seems to follow up the measurements at 8 GHz, while from transmission the losses from sample 14 are smaller than expected. Additional measurements have to be performed to clear up this point.

4. Conclusions

It was confirmed that infrared losses are not so sensitive to sample processing and that their extrapolation (both from transmission and reflectivity data) down to the microwave range is a useful procedure for estimating the intrinsic microwave losses.

It was also verified that fast cooling from high temperatures of $MgTiO_3$ samples (sample 3) causes an increase in overall losses of $MgTiO_3$ ceramics. A structural disorder in the material is proposed as responsible for the observed changes.

The additives can be classified into two types according to their effect. Those which lead to the formation of second phases and those which were maintained within the solid solution limits. Both of them affect the dielectric loss, but in a different way. In the first case, the influence on losses results from the combination of losses of each phase present and the effect on infrared losses is usually small. This is the case with La^{3+} and $CaTiO_3$ doping. In the second case, intrinsic losses can be quite markedly affected by the presence of the foreign elements in the lattice. The origin of the additional vibration mode damping is related to the anharmonic interaction of the lattice with imperfections (impurities, disorder). This is the case for doping with Cr^{3+}, Co^{2+} and Ni^{2+}. Doping with Nb^{5+} seems to be an intermediate situation.

References

1. K. WAKINO, M. MURATA and H. TAMURA, *J. Amer. Ceram. Soc.* **69** (1986) 34.
2. H. TAMURA, D. A. SAGALA and K. WAKINO, *Jpn. J. Appl. Phys.* **25** (1986) 787.
3. J. PETZELT *et al.*, *Ferroelectrics* **93** (1989) 77.
4. A. S. BARKER, Jr and M. TINKHAM, *Phys. Rev.* **125** (1962) 1527.
5. W. G. SPITZER, R. C. MILLER, D. A. KLEINMAN and L. E. HOWARTH, *ibid.* **126** (1962) 1710.
6. C. H. PERRY, D. J. MCCARTHY and G. O. RUPPRECHT, *Phys. Rev. A* **138** (1965) 1537.
7. G. O. RUPPRECHT and R. O. BELL, *Phys. Rev.* **125** (1962) 1915.
8. B. D. SILVERMAN, *ibid.* **125** (1962) 1921.
9. V. L. GUREVICH and A. K. TAGANTSEV, *Adv. Phys.* **40** (1991) 719.
10. J. PETZELT *et al.* in Proceedings of the 2nd European Conference on Polar Dielectrics, London, April 1992 (to be published in Ferroelectrics).
11. J. PETZELT *et al.*, *Phys. Rev. B* **30** (1984) 5172.
12. J. K. PLOURDE and C. L. REN, *IEEE Trans. Microwave Theory Tech.* **29** (1981) 754.
13. B. W. HAKKI and P. D. COLEMAN, *IRE Trans. Microwave Theory Tech.* **8** (1960) 402.
14. V. M. FERREIRA, F. AZOUGH, J. L. BAPTISTA and R. FREER in Proceedings of the 2nd European Conference on Polar Dielectrics, London, April 1992 (to be published in Ferroelectrics).
15. H. TAMURA and M. KATSUBE, US Patent 4242213, (1980).
16. A. M. F. Y. HAIDER and A. EDGAR, *J. Phys. C* **13** (1980) 6239.

Received 13 August 1992
and accepted 19 March 1993